Supporting Information

Liu et al. 10.1073/pnas.1420196111

SI Materials and Methods

Misacylation Assays. Wild-type and C723A human AlaRS were purified from *Escherichia coli* by affinity chromatography, and concentrations were determined by the Bradford assay (BioRad) and active site titration. Misacylation assays were performed at 25 °C in a reaction mixture of WT, C723A, or equal molar ratio of WT and C723A AlaRS at the concentrations as indicated with 50 mM Hepes (pH 7.5), 50 mM KCl, 4 mM ATP, 10 mM $MgCl_2$, 5 mM DTT, 4 ng/μL of inorganic pyrophosphatase (Roche), 10 μM ^{3}H-L-serine, 2 μM BSA, and 10 μM in vitro transcript corresponding to human $tRNA^{Ala}$. Assays were performed as described (1). Briefly, eight reactions were initiated simultaneously by mixing enzyme with a reaction mix in 96-well low-profile PCR plates. Samples were quenched in polyvinylidene fluoride (PVDF) MultiScreen filter plates containing 200 μL 5% TCA, 100 mM unlabeled serine, and 0.1% BSA as a carrier. Plates were washed 5 times with 5% TCA containing 100 mM serine followed by a one-time wash with 95% ethanol. Samples were liberated from the plate with 70 μL 100 mM NaOH, centrifuged into 150 μL of Supermix scintillant, and counted in a Microbeta plate reader. Assays were run in duplicate, and points (±SD) were averaged from two experiments.

Gene Targeting. The targeting cassette was constructed by two-step recombineering of a BAC (RP24-359N5) containing the *Aars* gene. To introduce the C723A mutation in *Aars* exon 15, exon 15 and flanking intronic sequences of 346 bp were cloned into a vector containing a neomycin resistance cassette flanked by Flp recombinase recognition target sites (FRT-neo-FRT). Site-directed mutagenesis (Stratagene) was used to change cysteine codon TGT to the alanine codon GCG. Replacement of wild-type *Aars* exon 15 by the mutated exon 15 was performed by BAC recombineering using *E. coli* strain SW105 (2). The neo cassette was excised by arabinose-induced Flp recombinase expression, leaving behind a single FRT site. Next, the loxP-stop-neo-loxP transcriptional stop cassette, with the transcriptional "STOP" sequence subcloned from pBS302 (Addgene), and a *neo* resistance gene under dual eukaryotic/prokaryotic promoter, was recombineered into intron 1 of the *Aars* gene in the BAC. The modified BAC was then linearized at two BsiWI sites in the BAC backbone and electroporated into C57BL/6J-$Tyr^{c\text{-}2J}$ ES cells. After G418 selection and colony expansion, Southern blot analysis was performed using a probe outside of the 5′ arm of the BAC to identify clones with the loxP-stop-neo-loxP cassette correctly targeted into *Aars* intron 1. To determine whether the mutated exon 15 was recombined into the *Aars* locus, long-range genomic PCR was performed and four of the six clones contained both the loxP-stop-neo-loxP cassette and the C723A mutation. ES cells were injected into C57BL6/J blastocysts, and the resulting chimeras were bred to C57BL/6J-$Tyr^{c\text{-}2J}$ mice.

Genotype Analysis. For preparing genomic DNA for PCR, a small piece of mouse tail was incubated at 95 °C for 15 min in 120 μL lysis buffer (50 mM NaOH), cooled down on ice, and then neutralized with 30 μL neutralization buffer (1 M Tris, 5 mM EDTA, pH 8.0). We used 1 μL crude genomic DNA for a 20-μL PCR. PCR was performed using the primer pairs to distinguish the wild-type *Aars* and $Aars^{C723A}$ alleles (stop-Cassette F2, 5′-CACTGCAGAGCACTACAGCAC-3′, and stop-Cassette R2, 5′-GTCTGTACCCACTGGCCTCT-3′). Wild-type and $Aars^{C723A}$ amplicons were 486 bp and 589 bp, respectively. To detect the $Aars^{stop}$ allele, PCR primers 4667F (5′-CCGCCTCAGGACTCTTCCTTT-3′) and stop-CassetteF2 were used that produced a 448-bp amplicon. PCR conditions were as follows: 35 cycles at 94 °C for 30 s, 60 °C for 30 s, and 72 °C for 40 s.

Histology. Mouse brain, skeletal muscle, liver, small intestine, kidney, liver, lung, and heart were immersion fixed in 10% neutral buffered formalin for 3 h, dehydrated, and embedded in paraffin. Sections 7 μm thick were deparaffinated, rehydrated, and stained with hematoxylin and eosin, Masson's trichrome, or picrosirius red staining according to standard procedures. Calbindin-D28 immnohistochemistry was performed as previously described (3). Cardiac fibrosis quantification was performed according to previously described methods (4). Basically, 8–10 longitudinal sections of the heart were taken at 100-μm intervals and stained with Masson's trichrome stain. Digitalized images (×200 magnification) were taken by Nanozoomer slide scanner, and fibrotic tissue (blue) and ventricular myocardium (red) were measured using a custom-made pipeline generated on CellProfiler. The percentage of fibrosis within a heart was calculated as the total fibrotic area divided by the total area. Perivascular collagen was excluded from analysis. For all histological analyses, at least four mice of each genotype and age were used.

Immunofluorescence. The following primary antibodies were used for immunofluorescence: rabbit anti-ubiquitin (1:1,000, # Z0458, DAKO), guinea pig anti-p62 (1:1,000, #03-GP62-C, ARP, Inc.), rabbit anti-LC3 (1:1,000, #PM036, MBL), rabbit anti-Hsp70 (1:100, #ADI-SPA-812-D, Enzo), and mouse anti-desmin (1:500, #D1033, Sigma). Detection was performed with Alexa Fluor-488– or -555–conjugated goat anti-mouse or rabbit secondary antibodies (1:200, Invitrogen). Sections were counterstained with Hoechst 33342, and autofluorescence was quenched with Sudan black.

Electron Microscopy. Mice fully anesthetized with tribromoethanol were transcardially perfused with phosphate-buffered saline, followed by 2% (wt/vol) paraformaldehyde and 2% (wt/vol) glutaraldehyde in cacodylate buffer (pH 7.2). Hearts were dissected and postfixed overnight in the same fixative. Transmission electron micrography (TEM) was performed according to standard procedures. TEM images were collected on a Jeol 1230 microscope.

Echocardiography. The Vevo 770 High-Frequency Ultrasound System (Visualsonics) was used to image cardiac morphology and to extrapolate cardiac function in anesthetized mice. For anesthetization, the animals were induced with 5% isoflurane at 1 L/min and maintained at 1.5% at 0.8 L/min. A complete cardiac examination was performed using the Vevo 707B RMV scanhead. The structure and function of the heart was quantified using 3 ultrasound modalities, B-mode, and M-mode. Images were used to assess cardiac function and anatomical defects by measuring the short axis of the left ventricle of the heart. Left ventricular posterior wall thickening (PWT) was calculated based on the following equation (5): PWT (%) = 100 * (PWs – PWd)/PWd. Septal thickening (ST) was calculated as ST (%) = 100 * (IVSs – IVSd)/IVSd.

Electrocardiogram. Cardiac electrical activity (electrocardiogram, ECG) signal acquisition was performed by the PowerLab System (AD Instruments). The animals were induced with 5% isoflurane at 1 L/min and maintained at 1.5% at 0.8 L/min. Pediatric leads were used in a three-lead configuration to acquire the electrical signals; the specific configuration used was Lead I based on Einthoven's Triangle. Recording of the ECG signal lasted for at

least 5 min (until a steady baseline signal was recorded for a 20–60-s interval). A median ECG tracing was derived by superimposing ECGs of 10 consecutive beats and was used to determine the following measurements: heart rate, the duration and amplitude of the P wave (representing atrial depolarization), the duration of the QRS complex (representing ventricular depolarization), the amplitude of the R wave (representing depolarization of main ventricular muscle mass), corrected QT interval (QTc, time taken for ventricular depolarization and repolarization corrected for heart rate), RR interval (time between two consecutive R waves), and PR interval (time from the onset of the P wave to the beginning of the QRS complex).

1. Beebe K, Waas W, Druzina Z, Guo M, Schimmel P (2007) A universal plate format for increased throughput of assays that monitor multiple aminoacyl transfer RNA synthetase activities. *Anal Biochem* 368(1):111–121.
2. Warming S, Costantino N, Court DL, Jenkins NA, Copeland NG (2005) Simple and highly efficient BAC recombineering using galK selection. *Nucleic Acids Res* 33(4):e36.
3. Liu Y, Zaun HC, Orlowski J, Ackerman SL (2013) CHP1-mediated NHE1 biosynthetic maturation is required for Purkinje cell axon homeostasis. *J Neurosci* 33(31):12656–12669.
4. Wolf CM, et al. (2005) Somatic events modify hypertrophic cardiomyopathy pathology and link hypertrophy to arrhythmia. *Proc Natl Acad Sci USA* 102(50):18123–18128.
5. Gao S, Ho D, Vatner DE, Vatner SF (2011) Echocardiography in mice. *Curr Protoc Mouse Biol* 1:71–83.

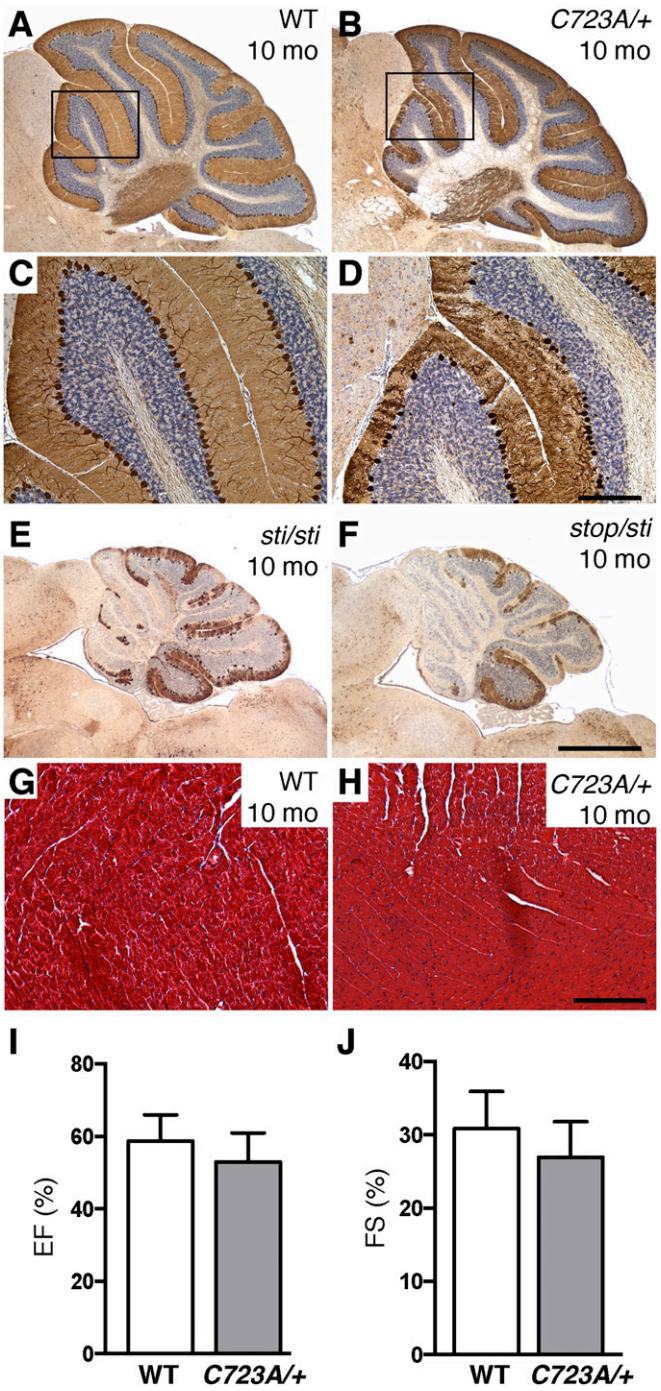

Fig. S1. Mild Purkinje cell degeneration and normal cardiac morphology and function in *Aars*$^{C723A/+}$ mice. (*A*–*F*) Calbindin D-28 immunohistochemistry (brown) on cerebellar sections of 10-mo-old wild-type (*A*), *Aars*$^{C723A/+}$ (*B*), *Aars*$^{sti/sti}$ (*E*), and *Aars*$^{stop/sti}$ (*F*) mice. (*C* and *D*) High-magnification images of the outlined regions in *A* and *B*, respectively. (*G* and *H*) Representative images of Masson's trichrome-stained heart sections from 10-mo-old wild-type (*G*) and *Aars*$^{C723A/+}$ (*H*) mice. (*I* and *J*) Ejection fraction (EF%; *I*) and fractional shortening (FS%; *J*) of 10-mo-old wild-type ($n = 5$) versus *Aars* $^{C723A/+}$ ($n = 5$) mice. [Scale bar, (*A*, *B*, *E*, and *F*) 1 mm, (*C* and *D*) 200 μm, and (*G* and *H*) 150 μm.]

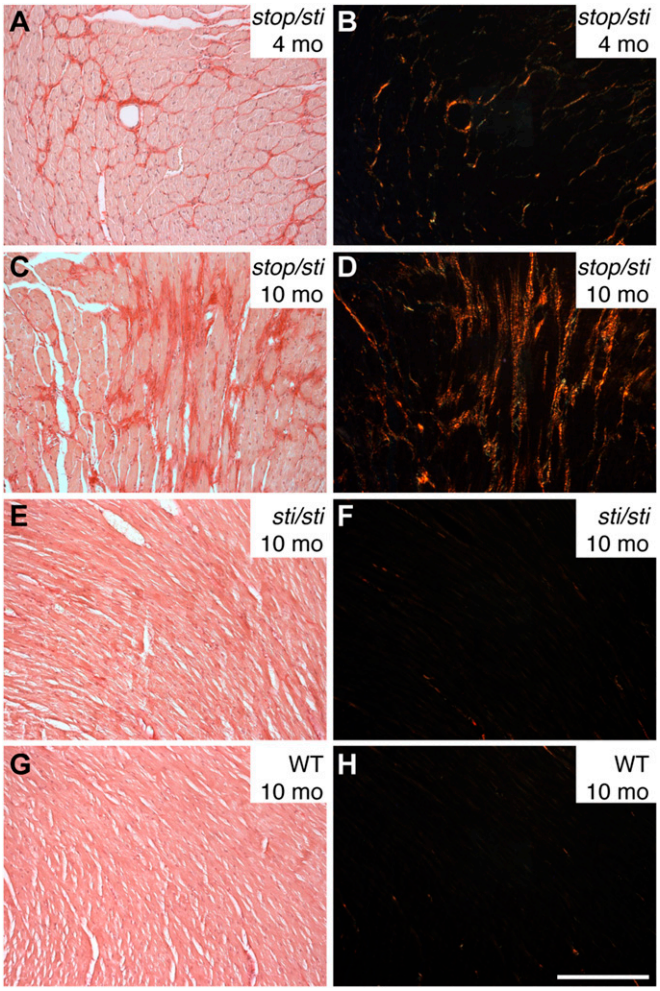

Fig. S2. Cardiac fibrosis in *Aars*$^{stop/sti}$ mice. Representative images of picrosirius red-stained heart sections from 4-mo-old *Aars*$^{stop/sti}$ (*A* and *B*), 10-mo-old *Aars*$^{stop/sti}$ (*C* and *D*), 10-mo-old *Aars*$^{sti/sti}$ (*E* and *F*), and 10-mo-old wild-type (*G* and *H*) mice. The same field was shown under bright field (*A*, *C*, *E*, and *G*) or circularly polarized light (*B*, *D*, *F*, and *H*). (Scale bar, 200 μm.)

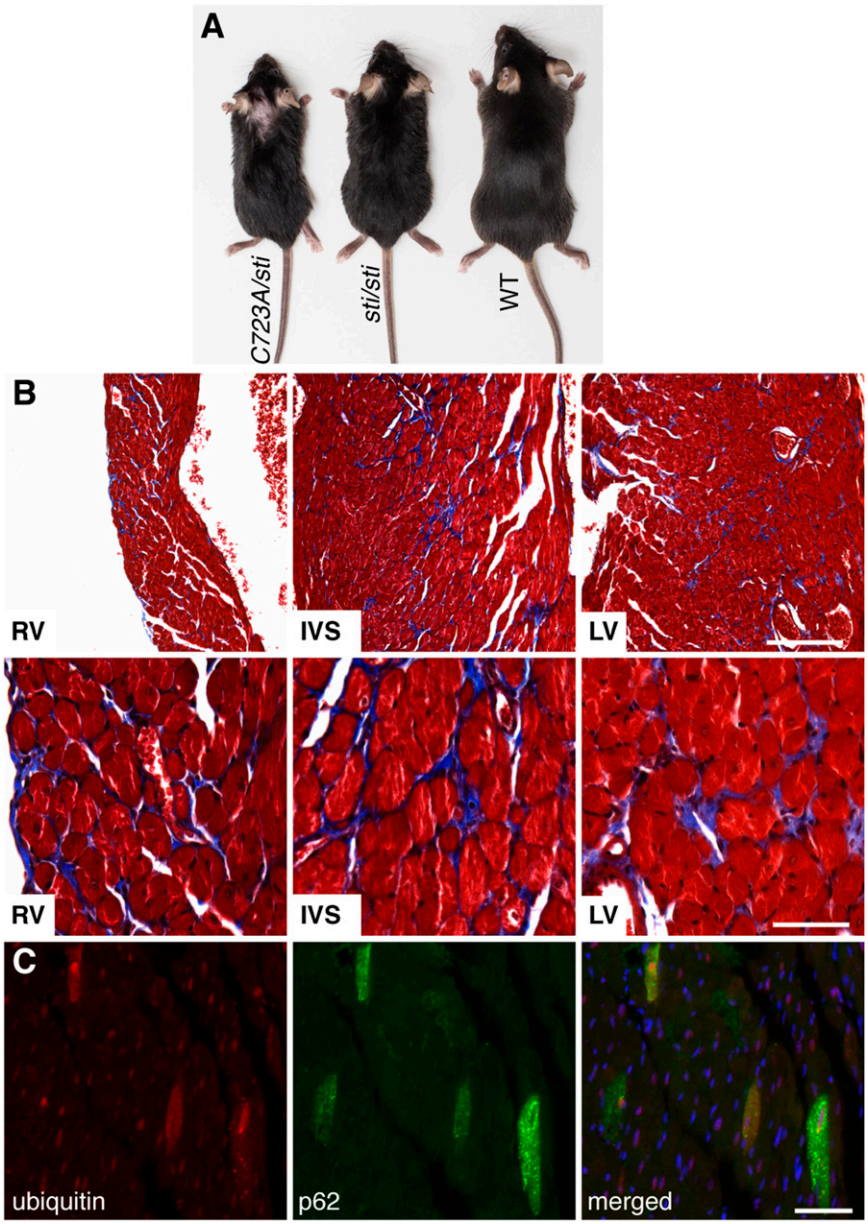

Fig. S3. *Aars*$^{C723A/sti}$ mice display small body size and cardiac proteinopathy. (*A*) Two-month-old *Aars*$^{C723A/sti}$ (*C723A/sti*), *Aars*$^{sti/sti}$ (*sti/sti*), and wild-type (WT) mice. Note the smaller body size and the dorsal alopecia of the *Aars*$^{C723A/sti}$ mouse. (*B*) Cardiac fibrosis (blue) in heart sections from 4-mo-old *Aars*$^{C723A/sti}$ mice revealed by Masson's trichrome stain. The *Lower* panel shows higher magnification images of representative areas from the *Upper* panel. IVS, interventricular septum; LV, left ventricular wall; RV, right ventricular wall. (Scale bar, 200 μm and 50 μm for *Upper* and *Lower* panels, respectively.) (*C*) Coimmunofluorescence of heart sections from 4-mo-old *Aars*$^{C723A/sti}$ mice with antibodies to ubiquitin (red) and p62 (green). Nuclei were stained with Hoechst 33342 (blue). (Scale bar, 50 μm.)

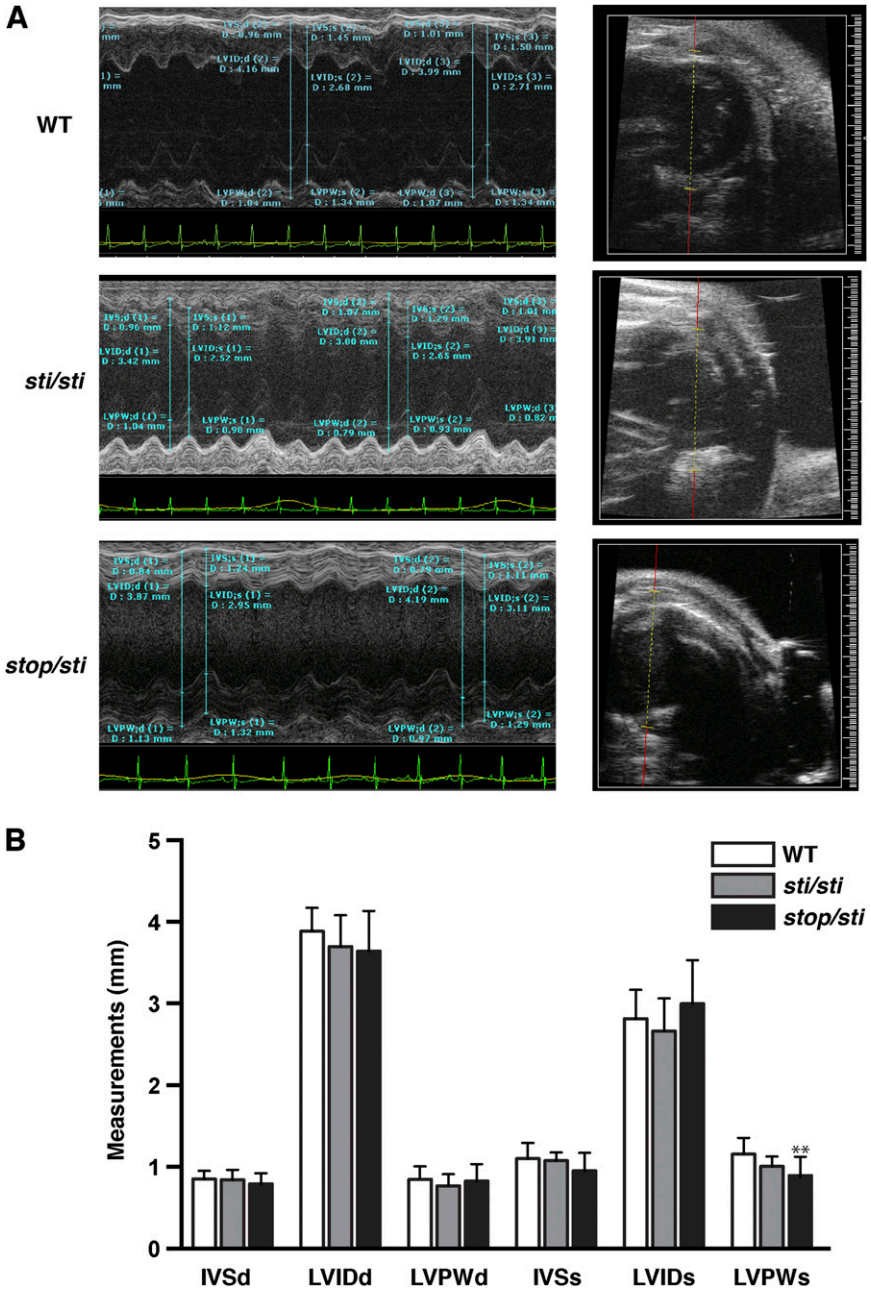

Fig. S4. Echocardiographic analysis of AlaRS editing-deficient mice. (*A*, *Left*) Representative M-mode echocardiographic images of 10-mo-old wild-type (WT), *Aars*$^{sti/sti}$ (*sti/sti*), and *Aars*$^{stop/sti}$ (*stop/sti*) mice. (*A*, *Right*) Left ventricle short axis view. (*B*) No significant difference was found across mouse strains for the following echocardiogram measurements in 10-mo-old *Aars*$^{stop/sti}$ ($n = 9$) or *Aars*$^{sti/sti}$ ($n = 6$) mice compared with wild-type ($n = 15$) mice: interventricular (IV) septum at diastole (IVSd), left ventricular (LV) internal dimension at diastole (LVIDd), LV posterior wall at diastole (LVPWd), IV septum at systole (IVSs), and LV internal dimension at systole (LVIDs). A small but significant decrease was found in the thickness of the LV posterior wall (LVPWs) of *Aars*$^{stop/sti}$ mice. Values are means ± SD. Data were analyzed by one-way ANOVA.

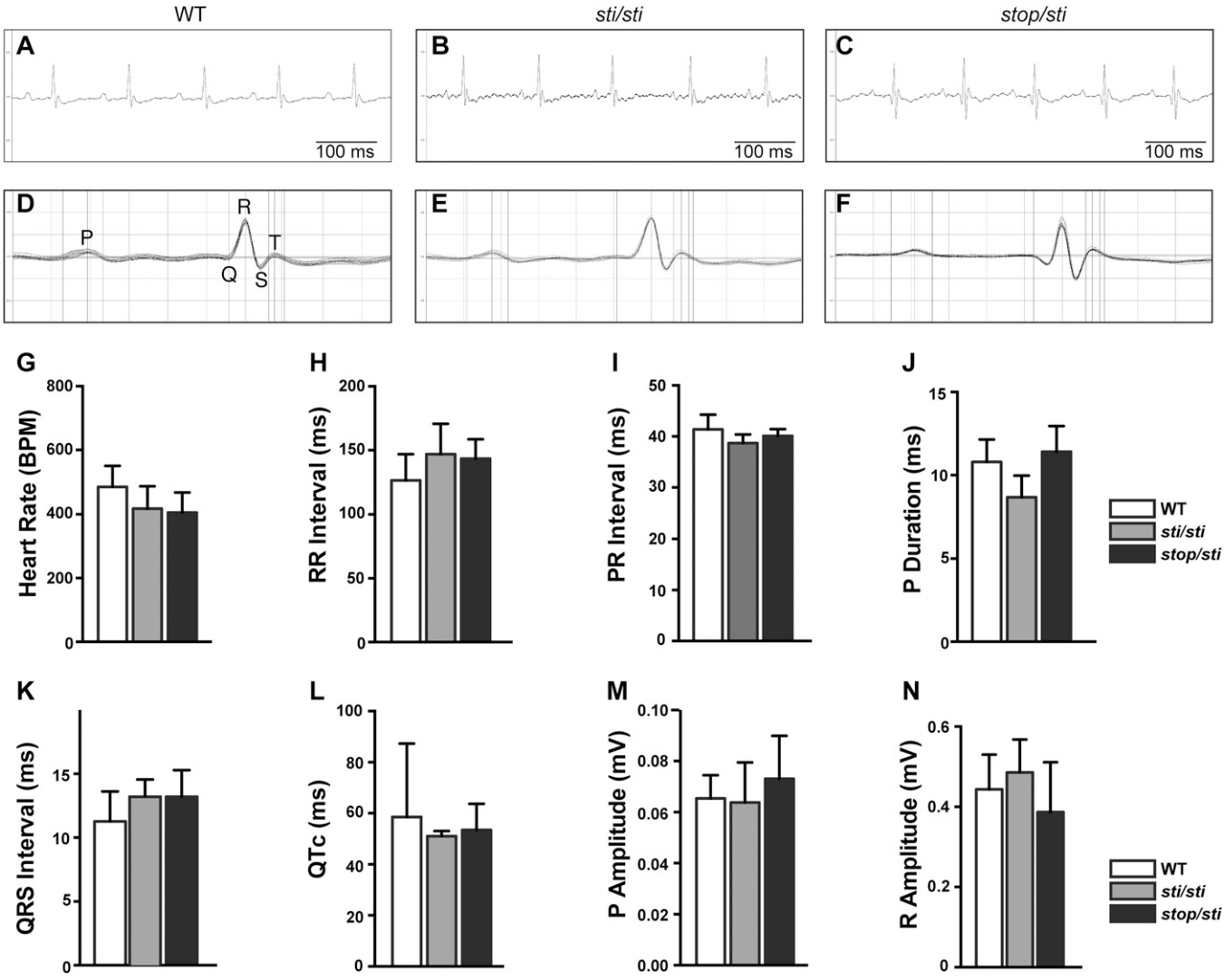

Fig. S5. Electrocardiographic analysis of AlaRS editing-deficient mice. (*A–F*) Representative electrocardiograms (ECGs) of wild-type (WT), *Aars*$^{sti/sti}$ (*sti/sti*), and *Aars*$^{stop/sti}$ (*stop/sti*) mice. The different waves (P, Q, R, S, T) that comprise the ECG are identified in *D*. (*G–N*) Values of ECG parameters (means ± SD) of 10-mo-old wild-type (WT; $n = 15$), *Aars*$^{sti/sti}$ (*sti/sti*; $n = 6$), and *Aars*$^{stop/sti}$ (*stop/sti*; $n = 9$) mice. No significant difference was found in ECG parameters between different genotypes (one-way ANOVA).

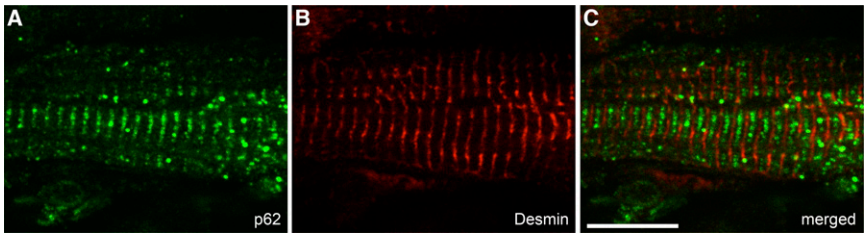

Fig. S6. Desmin is not a major component of protein aggregates in *Aars*$^{stop/sti}$ cardiomyocytes. (*A–C*) Coimmunofluorescence with antibodies to p62 (*A*) and desmin (*B*). Merged images are shown in *C*. (Scale bar, 10 μm.)

Table S1. Embryonic lethality of the *Aars*^{C723A} mutation

Age	Genotype of offspring		
	+/+	+/–	–/–
P7	12	22	0*
E10.5	3	7	0
E9.5	6	19	0*
E8.5	2	7	0

The number of embryos or pups with the given genotypes from *Aars*$^{C723A/+}$ intercross matings is shown.
*χ^2 analysis, 2 degrees of freedom, $P = 0.008$ ($\chi^2 = 9.64$) for embryonic day (E) 9.5 embryos; $P = 0.003$ ($\chi^2 = 11.41$) for postnatal day (P) 7 pups.

Table S2. Echocardiographic parameters of WT, *Aars*$^{sti/sti}$, and *Aars*$^{stop/sti}$ mice

Parameters	WT, $n = 15$	sti/sti, $n = 6$		stop/sti, $n = 9$	
	Mean ± SD	Mean ± SD	*P* value	Mean± SD	*P* value
IVSd, mm	0.85 ± 0.1	0.84 ± 0.12	0.99	0.79 ± 0.13	0.39
LVIDd, mm	3.88 ± 0.29	3.7 ± 0.38	0.49	3.64 ± 0.49	0.24
LVPWd, mm)	0.87 ± 0.14	0.77 ± 0.14	0.33	0.83 ± 0.21	0.77
IVSs, mm	1.1 ± 0.19	1.08 ± 0.1	0.95	0.95 ± 0.22	0.12
LVIDs, mm	2.82 ± 0.35	2.67 ± 0.4	0.68	3 ± 0.53	0.5
LVPWs, mm	1.16 ± 0.2	1.01 ± 0.12	0.24	0.89 ± 0.24	0.0087
% PWT	33.55 ± 16.77	33.19 ± 18.19	0.9983	7.31 ± 11.61	0.001
% ST	29.15 ± 13.01	29.23 ± 17.65	>0.9999	18.92 ± 13.07	0.1645
% EF	53.92 ± 7	55.05 ± 6.48	0.92	38.1 ± 7.71	<0.0001
% FS	27.63 ± 4.52	28.14 ± 3.97	0.96	18.08 ± 4.03	<0.0001